AIChE

Thermodynamics and Transport Properties of Citral

Nicolai Wörz and Peter Claus
Technische Universität Darmstadt, Ernst-Berl-Institut, Technische Chemie II, Darmstadt, Germany

Sebastian Lang and Manfred J. Hampe
Technische Universität Darmstadt, Institut für Thermische Verfahrenstechnik, Darmstadt, Germany

Petersenstraße 20, 64287 Darmstadt, Germany

DOI 10.1002/aic.12749
Published online October 11, 2011 in Wiley Online Library (wileyonlinelibrary.com).

In this work, transport and thermodynamic properties of mixtures of n-hexane with the aldehydes citral, citronellal and dihydrocitronellal, important to the fine chemicals industry, were determined experimentally and compared to theoretical predictions. Liquid binary diffusion coefficients were measured using the Taylor dispersion technique at various temperatures. The Wilke-Chang correlation gave precise approximations. The second part of this work is concerned with the gas-liquid phase equilibrium of citral/n-hexane. The mixture is slightly nonideal and may be sufficiently described by applying the modified UNIFAC (Dortmund) group contribution method. © 2011 American Institute of Chemical Engineers *AIChE J,* 58: 2557–2562, 2012
Keywords: citral, n-hexane, phase equilibrium, binary diffusion coefficient, Taylor dispersion

Introduction

Citral (CIT; 3,7-dimethyl-2,6-octadienal) belongs to the class of α,β-unsaturated aldehydes and may be used as a model substance for heterogeneously catalyzed selective hydrogenations.[1–4] Applying palladium as an active metal, hydrogenation of the carbonyl group is insignificant and the conjugated C=C bond is hydrogenated prior to the terminal isolated one.[5–8] This results in a simplified reaction network with citronellal (CAL) and dihydrocitronellal (DHC) as main products.[9] Physicochemical properties are scarce despite that citral and its hydrogenation products impact the fine chemicals and perfume industry.[10,11]

In view of modeling multiphase chemical reactions, plenty of thermodynamic and transport properties are necessary. Diffusivities must be determined in order to describe mass transport phenomena and their interplay with the catalytic reaction properly. Because of the extensive effort to measure binary diffusion coefficients experimentally, correlations[12–15] are frequently utilized to estimate them. Especially the Wilke-Chang[13] correlation is widely used and has already been applied for citral mixtures.[16–20] Unfortunately, correlations may differ extensively and without any experimental data it is difficult to choose reasonably. One aim of this study was to compare different correlations with experimentally determined binary diffusion coefficients using the dispersion technique originally proposed by Sir Geoffrey Taylor.[21–23]

Apart from transport properties, the thermodynamic behavior of the system *n*-hexane/citral was investigated. When modeling reaction kinetics, it is often convenient to formulate expressions of sources and sinks due to chemical reactions as a function of concentrations or mole fractions. In such cases all nonidealities are inevitably included into the regressed rate constants and this may possibly result in inaccurate models. To circumvent this drawback, rate expression may be written in terms of activities. It is then necessary to determine activity coefficients as a function of temperature, pressure and composition, which may be rather tedious especially in multicomponent systems. On the other hand, group contribution theories such as UNIFAC[24] and modified UNIFAC (Dortmund)[25] are sometimes adequate to describe the phase behavior but they might lead to completely wrong predictions. It is, therefore, highly advisable to verify estimations experimentally.

Equipment and Experimental Procedure

Materials

A mixture of *E*,*Z*-citral (> 97%) and *R*,*S*-citronellal (> 95%) was provided by Merck. The solvent *n*-hexane was supplied from Carl Roth in high purity (ROTIPURAN, > 99%). *R*,*S*-dihydrocitronellal (> 99%) was purchased from Essencia, Ätherische Öle AG. It is notable to mention that some compounds exhibit stereochemistry, but their discrimination shall not be considered within this article. The following notations: citral, citronellal, and dihydrocitronellal summarize all corresponding stereoisomers.

Description of the Taylor dispersion apparatus

All binary diffusion coefficients were measured using the Taylor dispersion apparatus shown in Figure 1. The device was designed in accordance with criteria given by Alizadeh

Additional Supporting Information may be found in the online version of this article.

Correspondence concerning this article should be addressed to P. Claus at claus@ct.chemie.tu-darmstadt.de.

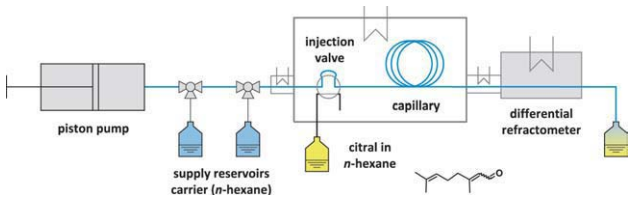

Figure 1. Schematic view of the Taylor dispersion apparatus.

[Color figure can be viewed in the online issue, which is available at wileyonlinelibrary.com.]

et al.[26] The carrier *n*-hexane was pumped with a syringe pump (ISCO 500D from Teledyne Isco, Inc.) with 0.1 mL min^{-1}. The capillary ($L = 10$ m, $r = 0.425$ mm, $d_L = 0.5$ m, PTFE), as well as the differential refractometer (WGE Dr. Bures GmbH and Co. KG) were situated in a thermostatic housing. Within a typical experiment, the carrier solution was pumped through the apparatus for at least 2 h until a constant base line could be observed. Then a pulse of solute in *n*-hexane was injected and the corresponding signal of the differential refractometer was recorded via LabVIEW™ (National Instruments, Corp.). In every case at least three runs were performed.

Fitting procedure

The radially-averaged concentration of component i at time t at the end of the tube relative to the background (carrier) concentration can be expressed as[27]

$$\bar{c}_i(t) = \frac{V_i c_{0,i}}{2\pi r^2} \frac{1}{\sqrt{\pi k t}} \exp\left[\frac{-L^2\left(1-\frac{t}{\tau}\right)^2}{4kt}\right] \tag{1}$$

with

$$k = \frac{r^2 L^2}{48\tau^2 D_{ij}} \tag{2}$$

Rearrangement leads to

$$\bar{c}_i(t) = \underbrace{\frac{V_i c_{0,i}}{2\pi r^2} \frac{\sqrt{48\tau^2}}{\sqrt{\pi r^2 L^2}}}_{f} \frac{\sqrt{D_{ij}}}{\sqrt{t}} \exp\left[-\frac{12 D_{ij}}{r^2}\frac{(\tau - t)^2}{t}\right] \tag{3}$$

In this equation f combines all time-independent variables and constant parameters except $\sqrt{D_{ij}}$. Assuming a linear dependency ($\gamma \equiv$ detector sensitivity) between the detector signal and the mean concentration and considering an offset α, a constant drift rate β and a noise $\epsilon(t)$

$$I_{\exp}(t) = \alpha + \beta t + \gamma \bar{c}_i(t) + \varepsilon(t) \tag{4}$$

the following fit-equation can be derived

$$I_{est}(t) = B_1 + B_2 t + B_3 \frac{\sqrt{B_4}}{\sqrt{t}} \exp\left[-\frac{12 B_4}{r^2}\frac{(B_5 - t)^2}{t}\right] \tag{5}$$

whereas $B_1 = \alpha$, $B_2 = \beta$, $B_3 = \gamma \cdot f$, $B_4 = D_{ij}$ and $B_5 = \tau$. It is possible to derive B_1, B_2 and B_5 directly from the measured data without including them into the fitting procedure. However, within this work very precise starting values for these parameters were determined manually first and a five parameter fit was performed to improve the quality of the fit. Figure 2 shows the results of a typical dispersion experiment. Fitting was accomplished with MATLAB® (The MathWorks, Inc.) applying the maximum likelihood solver.

Measurement of the phase equilibrium

The VLE data were obtained by the use of a Gillespie-type commercial equilibrium apparatus (VLE 602) produced by i-Fischer Engineering, Germany. The all-glass still is equipped with a Cottrell pump to ensure equilibrium between the vapor and liquid phase. The condensate and liquid were continuously recirculated into a mixing chamber, which was cooled by additional water quenching in order to prevent prompt evaporation of the volatile component *n*-hexane. This was necessary because of the high difference ($\Delta T_B \sim 159$ K) in boiling points of the two components. The equilibrium temperatures were measured by PT100 probes with an accuracy of 0.08 K. Nevertheless, the uncertainty of the temperature measurement could be as high as $\pm$ 0.5 K, because of concentration fluctuations due to inequalities during the recirculation. The pressure in the still can be set constant with an accuracy of $\pm$ 0.1 kPa according to the manufacturer. The apparatus can be operated at a temperature level of up to 493 K and in the pressure range from vacuum up to 400 kPa absolute pressure.

Isobaric VLE data were gathered by setting the still pressure constant and heating till a constant reflux rate of vapor and liquid phase was achieved. Samples of both phases were taken as soon as stationarity was reached. This was assumed after a change of the vapor phase temperature of less than 0.5 K within a time period of at least 10 min. The liquid phase concentration was changed either by adding a pure component or by removing *n*-hexane rich vapor phase through the sample outlet from the mixture. Thus, the VLE could be shifted in order to generate the data at various compositions. The compositions of the liquid and condensed vapor phase were determined by an Abbe refractometer (Atago 1230 NAR-3T), and a vibrating tube densimeter (Anton Paar DMA 5000) with an accuracy of $5 \cdot 10^{-2}$ kg m^{-3}. The results of both measuring methods were consistent.

The obtained data points were compared to predictive calculations of the vapor–liquid equilibrium. Three different

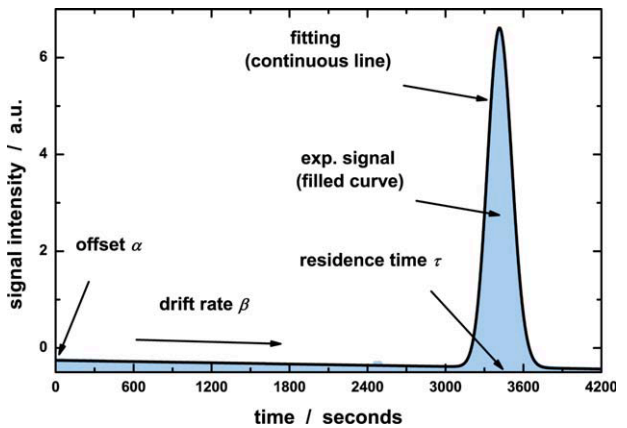

Figure 2. Illustration of the fitting procedure: filled (blue) curve: experimental data; continuous (black) line: fitting.

[Color figure can be viewed in the online issue, which is available at wileyonlinelibrary.com.]

Table 1. Experimental Diffusion Coefficients of Citral (CIT), Citronellal (CAL) and Dihydrocitronellal (DHC) at Infinite Dilution in *n*-Hexane

Solute -	Weight Percent[a] wt%	T K	D°_{ij}[b] 10^{-9} m^2 s^{-1}
CIT	1	293	2.61
CIT	3	283	2.29
CIT	3	293	2.54
CIT	3	303	2.82
CIT	3	308	3.11
CIT	5	293	2.49
CIT	5	303	2.69
CAL	3	293	2.46
DHC	3	293	2.43

[a]Weight percent of solute in *n*-hexane within the injection volume.
[b]Average of at least 3 runs.

methods were used. All calculations were performed under the assumption of ideal vapor phase behavior, which was justifiable due to the low-pressure level of 20 kPa. The liquid phase was first modeled as ideal, then with the predictive UNIFAC[24] group contribution method and the modified UNIFAC (Dortmund) method[25] developed by Gmehling and coworkers.

The pure component vapor pressure of citral, necessary for other calculations, was measured in the pressure range from 3 kPa up to 20 kPa in increments of 1-2 kPa. With these results the parameters for the extended Antoine equation (three parameters) were determined with the commercial software Aspen Plus® (Aspen Technologies, Inc.).

Results and Discussion

Binary diffusion coefficient

In Table 1. all measured binary diffusion coefficients are shown. All different runs and fittings of the same experiment present a relative standard deviation of about 3–4%. All values are in the range of typical liquid binary diffusion coefficients (10^{-9} m^2 s^{-1}). As expected, the diffusion coefficient increases with rising temperature. Besides, there is only a small difference among citral and its hydrogenation products citronellal and dihydrocitronellal, which is quite reasonable

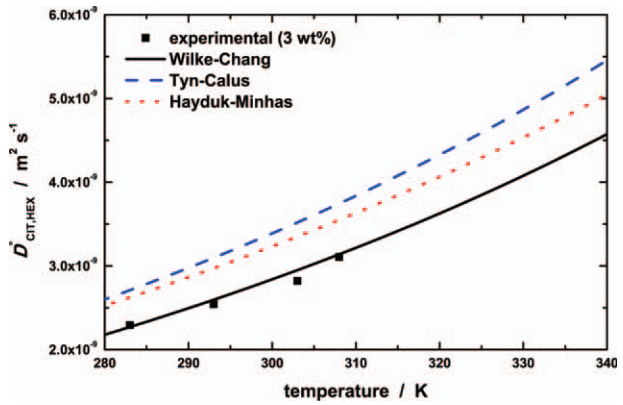

Figure 3. Comparison of various correlations with experimental binary diffusion coefficients: (■) experimental data; continuous (green) line: Wilke-Chang correlation[13]; dashed (blue) line: Tyn-Calus correlation[14]; dotted (red) line: Hayduk-Minhas correlation.[15]

[Color figure can be viewed in the online issue, which is available at wileyonlinelibrary.com.]

Table 2. Equations Used to Predict Binary Diffusion Coefficients at Infinite Dilution

Correlation	Equation	Comment
Wilke Chang[13]	$D^{\circ}_{ij} = \frac{7.4\cdot10^{-8}\left(\phi M_j\right)^{0.5} T}{\eta_j V_{m,i}^{0.6}}$	$\phi = 1$
Tyn and Calus[14]	$D^{\circ}_{ij} = 8.93\cdot10^{-8}\frac{V_{m,j}^{0.267}}{V_{m,i}^{0.433}}\frac{T}{\eta_j}$	for similar surface tensions
Hayduk and Minhas[15]	$D^{\circ}_{ij} = 13.3\cdot10^{-8}\frac{T^{1.47}\eta_j^{\left(10.2/V_i-0.791\right)}}{V_{m,i}^{0.71}}$	normal paraffin solutions

For further information and units compare Poling et al.[12]

regarding their structural resemblance. A slight decrease of the diffusion coefficient with increasing concentration of citral within the injection volume may be observed. The value at 3 wt % has been selected as reference because it exhibits distinct signal intensities, but can still be regarded as an infinitely dilute solution of citral in *n*-hexane. An entire investigation of the concentration dependency is very laborious and beyond the scope of this work.

Different correlations have been tested and compared to the experimental data (Figure 3). The corresponding equations are listed in Table 2. All properties concerning *n*-hexane are taken from Aspen Properties® (Aspen Technologies, Inc.). In case of citral, the liquid molar volume at its normal boiling point is calculated according to

$$V_{m,CIT}[m^3 mol^{-1}] = \frac{R[J\,mol^{-1}\,K^{-1}]T_c[K]\left(Z_{RA}^{[1+(1-T_r)^{2/7}]}\right)}{p_c[Pa]} \quad (6)$$

whereas T_c = 699 K and p_c = 22.9·10^5 Pa were determined applying the Lydersen estimation method[18,28] with T_B = 501 K. The Racket parameter Z_{RA} = 0.2236 was obtained by regressing density data at various temperature levels.

Based on our studies, the binary diffusion coefficient of citral in *n*-hexane can be estimated quite accurately using the Wilke-Chang correlation (deviation < 5%). Even the temperature dependence seems to be predicted very precisely. The Tyn-Callus and the Hayduk-Minhas method are acceptable approximations as well, but exhibit small offsets toward higher values over the whole temperature range. One explanation may be that these equations are already

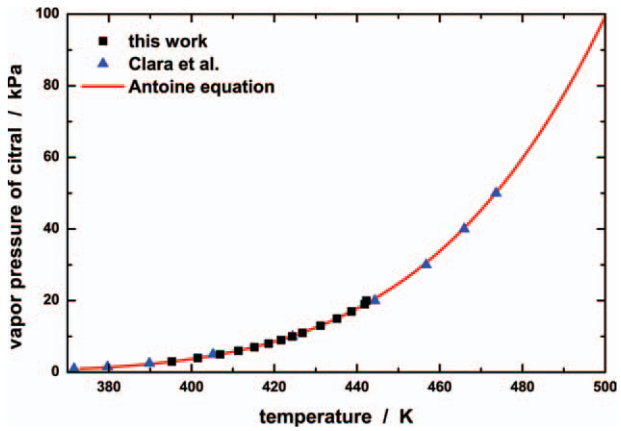

Figure 4. Vapor pressure of citral: (■) experimental data of this work; (▲) Clará et al.[29]; continuous (red) line: regressed Antoine equation.

[Color figure can be viewed in the online issue, which is available at wileyonlinelibrary.com.]

Table 3. Vapor Pressure Data of Measured Pure Citral

T K	p_{vp} kPa
395.2	3
401.5	4
406.9	5
411.3	6
415.2	7
418.6	8
421.7	9
424.3	10
426.8	11
431.2	13
435.2	15
438.7	17
441.9	19
442.3	20

simplifications for components with similar surface tensions and normal paraffin solutions, respectively (Table 2).

Phase equilibrium and activity coefficients

Figure 4 presents the regressed vapor pressure curve of the pure component citral. The regressed curve is in excellent agreement with the experimental data from this work and from Clara et al.[29] The curve was plotted according to the following three-parametric Antoine equation

$$p_{vp}[\mathrm{Pa}] = \exp\left[C_1 + \frac{C_2}{T[\mathrm{K}] + C_3}\right] \tag{7}$$

The parameters C_1 to C_3 were obtained by regression using the experimental data listed in Table 3. The parameters are: $C_1 = 20.4 \pm 0.4$; $C_2 = -3298.8 \pm 255.5$, and $C_3 = -129.5 \pm 11.9$.

Figure 5 presents the experimental data for the vapor–liquid measurement of *n*-hexane and citral at 20 kPa, as well as the predictive calculations. Ideality was assumed for the vapor phase in all cases. Hence, there is only one dew point curve to examine, which slightly underpredicts the actual behavior. The bubble-point curve calculated according to

Table 4. Experimental Vapor–Liquid Equilibrium Data for *n*-Hexane and Citral at 20 kPa

T K	x_{CIT} –	x_{HEX} –	y_{CIT} –	y_{HEX} –
298.2	0.000	1.000	0.000	1.000
299.3	0.004	0.996	0.004	0.996
300.3	0.151	0.849	0.003	0.997
300.5	0.145	0.855	0.004	0.996
301.4	0.217	0.783	0.002	0.998
302.1	0.277	0.723	0.004	0.996
304.3	0.454	0.546	0.004	0.996
305.1	0.182	0.818	0.005	0.995
305.3	0.488	0.512	0.005	0.995
307.6	0.520	0.480	0.006	0.994
311.9	0.489	0.511	0.005	0.995
327.7	0.856	0.144	0.011	0.989
336.0	0.885	0.115	0.005	0.995
346.9	0.921	0.079	0.014	0.986
347.5	0.927	0.073	0.005	0.995
360.9	0.914	0.086	0.028	0.972
379.9	0.978	0.022	0.018	0.982
400.1	0.936	0.064	0.158	0.842
435.2	0.961	0.039	0.648	0.352
438.3	1.000	0.000	0.735	0.265
442.3	1.000	0.000	1.000	0.000

Raoult's law has the highest deviation and is obviously overestimating the temperature. The UNIFAC and especially the modified UNIFAC (Dortmund) model make more realistic predictions. As the standard UNIFAC model still seems to overestimate the characteristics of the bubble point curve, we recommend the use of the modified UNIFAC (Dortmund) model as predictive method. This can be explained by the better ability of the UNIFAC (Dortmund) model to characterize strongly temperature-dependent mixtures.[25] Table 4 shows the experimental vapor–liquid equilibrium data for *n*-hexane and citral at 20 kPa. Steady-state conditions were difficult to achieve at high-citral mole fractions (> 0.8). Furthermore, polymerization can be an issue at such high temperatures. We did not check for the production of oligomers or polymers, but when keeping high temperatures for a long time, a change in color to intensive yellow was observed.

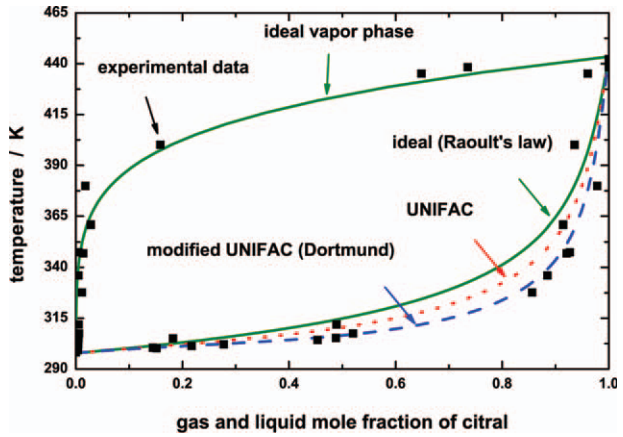

Figure 5. *T*(*x*,*y*) diagrams for *n*-hexane and citral at 20 kPa: (■) experimental data; continuous (green) line: ideal Raoult's law; dotted (red) line: UNIFAC; dashed (blue) line: modified UNIFAC (Dortmund).

[Color figure can be viewed in the online issue, which is available at wileyonlinelibrary.com.]

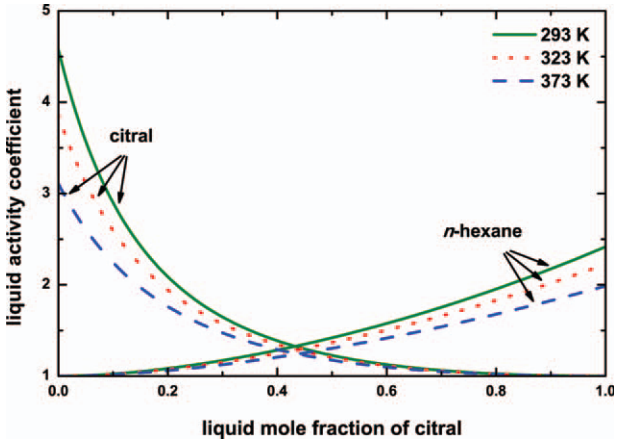

Figure 6. Predicted liquid activity coefficients for *n*-hexane and citral according to the modified UNIFAC (Dortmund) group contribution method: continuous (green) line at 293 K; dotted (red) line at 323 K; dashed (blue) line at 373 K.

[Color figure can be viewed in the online issue, which is available at wileyonlinelibrary.com.]

Figure 6 illustrates the predicted liquid activity coefficients for *n*-hexane and citral for three different temperature levels (293, 323 and 373 K). The limiting activity coefficient of citral lies in the region of 4.5 whereas the one of *n*-hexane reaches only about 2.5 at 293 K. Both activity coefficients show a small positive deviation from ideal behavior. The activity coefficients in the liquid phase decrease for both components with increasing temperature.

Conclusion

Liquid binary diffusion coefficients of citral, citronellal and dihydrocitronellal were measured at various temperatures using the Taylor dispersion technique. All values of diffusion coefficients were in typical range and the overall relative standard deviation was below 4%. Citral, citronellal and dihydrocitronellal exhibit similar diffusion coefficients, which seems reasonable in view of their structural analogy. The Wilke-Chang correlation allows a precise prediction of the measured diffusion coefficients and their temperature dependence, whereas the methods from Tyn-Calus and Hayduk-Minhas show small offsets to higher values.

In the second part of this study, the vapor–liquid phase equilibrium of the system citral/*n*-hexane was examined. It was possible to analyze the entire range of molar compositions at 20 kPa. The liquid system is slightly nonideal and might be described with the modified UNIFAC (Dortmund) group contribution method. The gas phase shows ideal gas behavior as might have been expected at low pressures.

In conclusion, it could be stated that binary mixtures of citral and some of its hydrogenation products in *n*-hexane could be described with predictive methods in view of mutual diffusion coefficients and gas-liquid phase equilibrium. Hence, no further regression methods have to be carried out inside the range studied.

Notation

a.u. = arbitrary units
$B_1 - B_5$ = fitting parameters
$\bar{c}_i(t)$ = radially-averaged concentration of component i at time t at the end of the tube relative to the background (carrier) concentration
CAL = *R*,*S*-citronellal
CIT = *E*,*Z*-citral
DHC = *R*,*S*-dihydrocitronellal
D_{ij} = binary diffusion coefficient of solute i in solvent j
D_{ij}° = binary diffusion coefficient of solute i at infinite dilution in solvent j
d_L = loop diameter of the capillary
HEX = *n*-hexane
I_{est} = estimated intensity
I_{exp} = experimental intensity
L = length of the capillary
p_c = critical pressure
p_{vp} = vapor pressure
r = radius of the capillary
R = ideal gas constant
T = temperature
T_B = normal boiling point
T_c = critical temperature
$V_i c_{0,i}$ = number of moles of component i in the injection pulse
V_m = liquid molar volume
VLE = vapor–liquid equilibrium
wt % = weight percent
x = liquid mole fraction, mol mol^{-1}
y = vapor mole fraction, mol mol^{-1}
Z_{RA} = Rackett parameter

Greek letters

α = detector offset
β = drift rate
γ = detector sensitivity
ϵ = signal noise
τ = residence time
ϕ = association factor
η = liquid viscosity

Literature Cited

1. Claus P. Selective hydrogenation of α,β-unsaturated aldehydes and other C=O and C=C bonds containing compounds. *Top Catal*. 1998;5:51–62.
2. Gallezot P, Richard D. Selective hydrogenation of α,β-unsaturated aldehydes. *Catal Rev Sci Eng*. 1998;40:81–126.
3. Mäki-Arvela P, Hájek J, Salmi T, Murzin DY. Chemoselective hydrogenation of carbonyl compounds over heterogeneous catalysts. *Appl Catal A*. 2005;292:1–49.
4. Claus P, Önal Y.*Regioselective Hydrogenations*. In:Ertl G,Knözinger H,Schüth F,Weitkamp J. *Handbook of Heterogeneous Catalysis*. 2nd ed. Weinheim: Wiley-VCH; 2008:3308–3329.
5. Aramendía MA, Borau V, Jiménez C, Marinas JM, Porras A, Urbano FJ. Selective liquid-phase hydrogenation of citral over supported palladium. *J Catal*. 1997;172:46–54.
6. Liu R, Yu Y, Yoshida K, Li G, Jiang H, Zhang M, Zhao F, Fujita S, Arai M. Physically and chemically mixed TiO_2-supported Pd and Au catalysts: unexpected synergistic effects on selective hydrogenation of citral in supercritical CO_2. *J Catal*. 2010;269:191–200.
7. Satagopan V, Chandalia SB. Selectivity aspects in the multi-phase hydrogenation of α,β-unsaturated aldehydes over supported noble metal catalysts: Part I. *J Chem Tech Biotechnol*. 1994;59:257–263.
8. Hao J, Xi C, Cheng H, Liu R, Cai S, Arai M, Zhao F. Influence of compressed carbon dioxide on hydrogenation reactions in cyclohexane with a Pd/C catalyst. *Ind Eng Chem Res*. 2008;47:6796–6800.
9. Wörz N, Arras J, Claus P. Continuous selective hydrogenation of citral in a trickle-bed reactor using ionic liquid modified catalysts. *Appl Catal A*. 2011;391:319–324.
10. Bröcker F, Kaibel G, Aquila W, Fuchs H, Wegner G, Stroezel M. Verfahren zur selektiven Flüssigphasenhydrierung von alpha-beta-ungesättigten Carbonylverbindungen. European Patent 0 947493 A1, 1999.
11. Göbbel H, Gerlach T, Funke F, Ebel K, Unverricht S, Kaibel G. Verfahren zu selektiven Hydrierung von olefinischen ungesättigten Carbonylverbindungen. European Patent 1 318128 A2, 2003.
12. Poling BE, Prausnitz JM,O'Connell JP. *The Properties of Gases and Liquids*. 5th ed. McGraw-Hill; 2004.
13. Wilke CR, Chang P. Correlation of diffusion coefficients in dilute solutions. *AIChE J*. 1955;1:264–270.
14. Tyn MT, Calus WF. Diffusion coefficients in dilute binary liquid mixtures. *J Chem Eng Data*. 1975;20:106–109.
15. Hayduk W, Minhas BS. Correlation for prediction of molecular diffusivities in liquids. *Can J Chem Eng*. 1982;60:295–299.
16. Aumo J, Wärnå J, Salmi T, Murzin DY. Interaction of kinetics and internal diffusion in complex catalytic three-phase reactions: Activity and selectivity in citral hydrogenation. *Chem Eng Sci*. 2006;61:814–822.
17. Mikkola JP, Wärnå J, Virtanen P, Salmi T. Effect of internal diffusion in supported ionic liquid catalysts: Interaction with kinetics. *Ind Eng Chem Res*. 2007;46:3932–3940.
18. Mukherjee S, Vannice MA. Solvent effects in liquid-phase reactions: I. Activity and selectivity during citral hydrogenation on Pt/SiO_2 and evaluation of mass transfer effects. *J Catal*. 2006;243:108–130.
19. Steffan M. Heterogen katalysierte Selektivhydrierung von Citral in der Flüssigphase. [PhD Thesis]. Darmstadt University of Technology, Germany; 2008.
20. Önal Y. Reaktionstechnische Aspekte der wässrigen Mehrphasenkatalyse: Von Grundlagen-Untersuchungen über innovatives Reaktordesign bis zur kinetischen Modellierung. [PhD Thesis]. Darmstadt University of Technology, Germany; 2005.
21. Taylor G. Dispersion of soluble matter in solvent flowing slowly through a tube. *Proc R Soc Lond A*. 1953;213:186–203.
22. Taylor G. The dispersion of matter in turbulent flow through a pipe. *Proc R Soc Lond A*. 1954;223:446–468.
23. Taylor G. Conditions under which dispersion of a solute in a stream of solvent can be used to measure molecular diffusion. *Proc R Soc Lond A*. 1954;225:473–477.

24. Fredenslund A, Jones RL, Prausnitz JM. Group-contribution estimation of activity coefficients in nonideal liquid mixtures. *AIChE J*. 1975;21:1086–1099.
25. Weidlich U, Gmehling J. A modified UNIFAC Model. 1. Prediction of VLE, h^E, and γ^∞. *Ind Eng Chem Res*. 1987;26:1372–1381.
26. Alizadeh A, Nieto de Castro CA, Wakeham WA. The theory of the taylor dispersion technique for liquid diffusivity measurements. *Int J Thermophys*. 1980;1:243–284.
27. Van de Ven-Lucassen IMJJ, Kieviet FG, Kerkhof PJAM. Fast and convenient implementation of the Taylor dispersion method. *J Chem Eng Data*. 1995;40:407–411.
28. Lydersen AL. Estimation of Critical Properties of Organic Compounds. University of Wisconsin College of Engineering, Eng., Exp. Stn. rept. 3. Madison, WI; 1995.
29. Clará RA, Gómez Marigliano AC, Sólimo HN. Density, viscosity, and refractive index in the range (283.15 to 353.15) K and vapor pressure of α-pinene, *d*-limonene, (±)-linalool, and citral over the pressure range 1.0 kPa atmospheric pressure. *J Chem Eng Data*. 2009;54:1087–1090.

Manuscript received Dec. 14, 2010, revision received May 27, 2011, and final revision received Aug. 2, 2011.